Arons and Diepen (2). This system exhibits gas-gas equilibria of the same type as observed in the helium–*n*-butane system. The bubble point curves in this system indeed open out in the manner postulated in Figure 3 as the helium concentration increases (see Figure 6 of reference 2). Isothermal retrograde condensation of the second kind was also observed in this system for several mixtures rich in xenon. It must be concluded that the type of phase behavior observed in the helium–*n*-butane system is typical of binary systems containing helium and a much heavier fluid. This type of gas-gas equilibrium, then, must result from the large disparity in size and intermolecular energy of the component molecules. This question is examined further in Part II.

LITERATURE CITED

1. Altemose, V. O., *J. Appl. Phys.*, **32**, 1909 (1961).
2. Arons, J. De Swaan, and G. A. M. Diepen, *J. Chem. Phys.*, **44**, 2322 (1966).
3. Aroyan, H. J., and D. L. Katz, *Ind. Eng. Chem.*, **43**, 185 (1951).
4. Buzyna, G., R. A. Macriss, and R. T. Ellington, *Chem. Engr. Progr. Symp. Ser. No. 44*, **59**, 101 (1963).
5. Jones, A. E., Ph.D. dissertation, Ohio State Univ., Columbus (1964); Dissertation Abstracts Order No. 1192 Microfilm $3.05, University Microfilms Inc., 313 N. 1st St., Ann Arbor, Mich.
6. Kamerlingh-Onnes, H., and W. H. Keesom, *Kon. Akad. Wetensch. Proc. Sect. Sci.*, **9**, 786; **10**, 231 (1907).
7. Kay, W. B., *Chem. Rev.*, **29**, 501 (1941).
8. ———, and W. E. Donham, *Chem. Eng. Sci.*, **4**, 1 (1953).
9. Kay, W. B., and G. M. Rambosek, *Ind. Eng. Chem.*, **45**, 221 (1953).
10. Krichevskii, I. R., and P. E. Bolshakov, *Zh. Fiz. Khim.*, **15**, 184 (1941).
11. Ostrovskii, I. A., *ibid.*, **37**, 942 (1963).
12. Tsiklis, D. S., *Dokl. Akad. Nauk SSSR*, **86**, 1159 (1952).
13. *Ibid.*, **91**, 1361 (1953).
14. ———, Termodinam i Stroenie Rastvorov Akad. Nauk. SSR, Otel. Khim. Nauk i Khim. Fak., Moskov. Gosudarst, Univ., Trudy Soveshch., p. 193, Moscow (1958).
15. Urbakh, V. Yu., *Zh. Fiz. Khim.*, **32**, 1163 (1958).

Manuscript received August 4, 1965; revision received November 14, 1966; paper accepted November 14, 1966.

Part II. Second Virial Coefficients for Helium—*n*-Butane Mixtures

The second virial coefficients of pure *n*-butane and of two mixtures of helium and *n*-butane were determined in the range 100° to 225°C. from isothermal compressibility measurements. Values of B_{11} (pure *n*-butane) agree closely with those of McGlashan and Potter *(11)* at low temperatures and of Hirschfelder et al. *(7)* at higher temperatures. Values of the mixed second virial coefficient B_{12} were computed from the mixture data. B_{12} shows little variation with temperature over this interval. The interpretation of the data as the behavior of a mixture composed of hard sphere (helium) in a real gas (*n*-butane) is discussed.

The occurrence of the gas-gas equilibrium, observed in the helium–*n*-butane system (see Part I), can be qualitatively ascribed to the large differences in the molecular sizes and energies of the two components. However, a more quantitative description of the intermolecular forces in this system is desirable when examining its phase behavior. It was decided therefore to include in our experimental program the determination of B_{12}, the mixed second virial coefficient representing the interaction of a helium atom with a molecule of *n*-butane.

The second virial coefficients of pure *n*-butane, B_{11}, and of the two helium–*n*-butane mixtures containing 35.3 and 38.3 mole % helium, respectively, were determined at six temperatures in the range 100° to 225°C. from isothermal compressibility measurements of the superheated vapor. Measurements were made in a range of densities from 0.1 to 0.5 mole/liter. Values of the second virial coefficient of helium B_{22} were obtained from the work of Schneider and Duffie (17).

EXPERIMENTAL PROCEDURE

As in the phase and volumetric measurements reported in Part I, the fluid sample was confined over mercury in a glass tube surrounded by a constant-temperature jacket. A sample

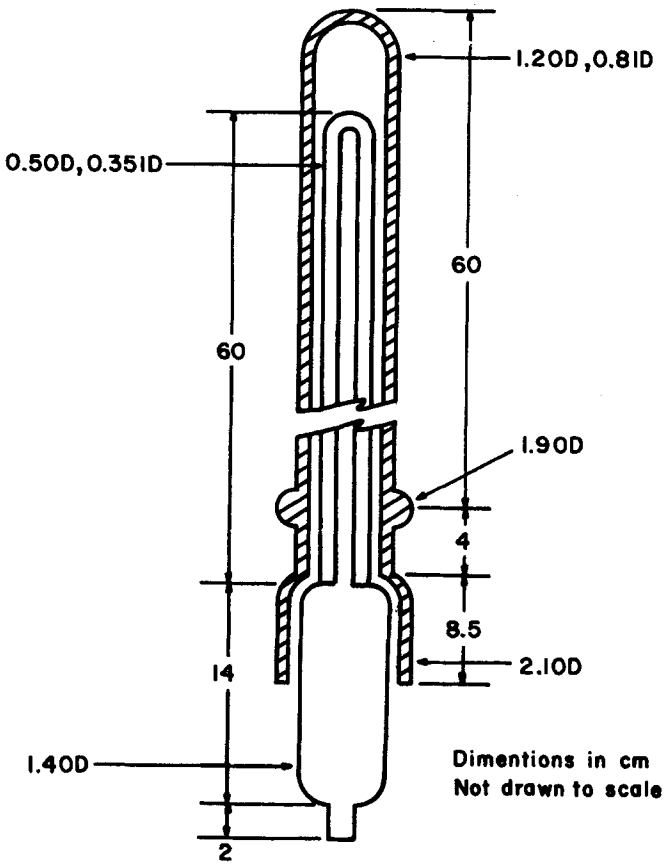

Fig. 1. Low-pressure sample tube.

tube of novel design, Figure 1, was used to contain the relatively large volumes of the gas when at low pressures. A thin-walled tube of soda-lime glass was used as the sample tube and was placed inside a heavy-walled borosilicate tube which was fastened in the compressor block. The inner sample tube floated in mercury and the annular space between the two tubes was filled with a helium-air mixture of the same partial pressure of helium as the sample. The driving force of helium diffusion was thus greatly diminished; measurements of the mass of sample before and after each set of experimental runs indicated no measurable loss. The tube design also eliminated the troublesome volume correction due to the pressure expansion of the sample tube.

The temperature of the vapor bath surrounding the sample tube was measured to within 0.01°C. by the same copper-constantan thermocouple described in Part I. However, a more precise dead weight gauge with a sensitivity of 0.01 lb./sq. in. was used for the pressure measurements. Corrections to the observed pressure were made for the difference in mercury levels in the apparatus, the capillarity of the mercury meniscus, and the vapor pressure of mercury. The precision of the pressure determination was ±0.014 lb./sq. in. or one part in 4,000 at the lowest pressure. The sample volume was determined from measurements of the length of the tube occupied by the sample by using a cathetometer reading to 0.001 mm. The precision of the volume determination was $\pm 2.2 \times 10^{-4}$ cc., or one part in 2,000 at the smallest volume.

The sample mass and composition were determined from the isothermal compressibility measurements themselves. The data, to within their experimental uncertainty, could be represented by a truncated virial equation:

$$\frac{PV}{nRT} = \frac{Bn}{V} \frac{Cn^2}{V^2} \qquad (1)$$

Equation (1) may be rearranged to give for each data point

$$y_i \equiv \left(\frac{P_i V_i}{nRT} - 1 \right) \frac{V_i}{n} = B + \frac{Cn}{V_i} \qquad (2)$$

Values of B, C, and n were obtained from a set of isothermal compressibility measurements by minimizing the sum of the squares of the deviations of all experimental points from the regression line given by Equation (2). The calculations were performed on an 7090 IBM computer.

The sequence of experimental measurements was as follows: First, n-butane was loaded in the sample tube which was then fastened in the compressor block. A check of the sample purity was made as in Part I. Isothermal compressibility measurements of the n-butane were then made at two or more temperatures. At each temperature. a value of n, the number of moles of sample, was obtained as outlined above. In all cases the agreement in the values of n was one part in 1,000 or better. An average of the values was taken as the number of moles of n-butane (n_1). The sample tube was then removed from the compressor block and helium was added to give a mixture of approximately the desired composition. The sample tube was replaced, and compressibility measurements of the mixture were made at 100°, 125°, 150°, 175°, 200°, and 225°C. The average of the number of moles of mixture computed for each isotherm was taken as $n_1 + n_2$, the total moles of mixture. The composition was thus obtained with a precision of 0.1 mole %. Additional details of the experimental apparatus and procedure are given elsewhere (9).

EXPERIMENTAL RESULTS

The experimental compressibility data for pure n-butane and for the two helium–n-butane mixtures are given in Tables 1† and 2,† respectively. The data for each isotherm cover an approximate range of densities from 0.1 to 0.5 moles/liter only, due to limitations imposed by the sample configuration. This density range does not extend high enough to obtain meaningful values of the third virial coefficient C from these data.

SECOND VIRIAL COEFFICIENT OF n-BUTANE, B_{11}

The second virial coefficient of pure n-butane, computed from the data as described above, is presented in Table 3 and in Figure 2, together with data reported by other investigators. The precision of each of the experimental values, as determined from a regression analysis, is ± 2.0 cc./g.-mole or less. The experimental values may be represented by the equation

$$B_{11}(T) = 1311.06 - 1.07795\,T - \frac{499813}{T} \text{ (cc./g.-mole)} \qquad (3)$$

with a maximum deviation of less than 1.0%.

Values of B_{11} given by Hirschfelder et al. (7), calculated from the data of Beattie et al. (1) at 150°C. and above, are in good agreement. McGlashan and Potter (11) report values of B_{11} at temperatures up to 140°C. The present results agree closely with their values at the

† Deposited as document 9440 with the American Documentation Institute, Photoduplication Service, Library of Congress, Washington 25, D. C., and may be obtained for $1.25 for photoprints or 35-mm. microfilm.

Table 3. Experimental Values of the Second Virial Coefficient of n-Butane

T, °K.	B_{11}, cc./g.-mole
368.25	—444.2
373.22	—429.5
378.18	—418.0
398.14	—376.0
423.14	—326.1
448.18	—284.8
473.21	—256.3
498.20	—228.7

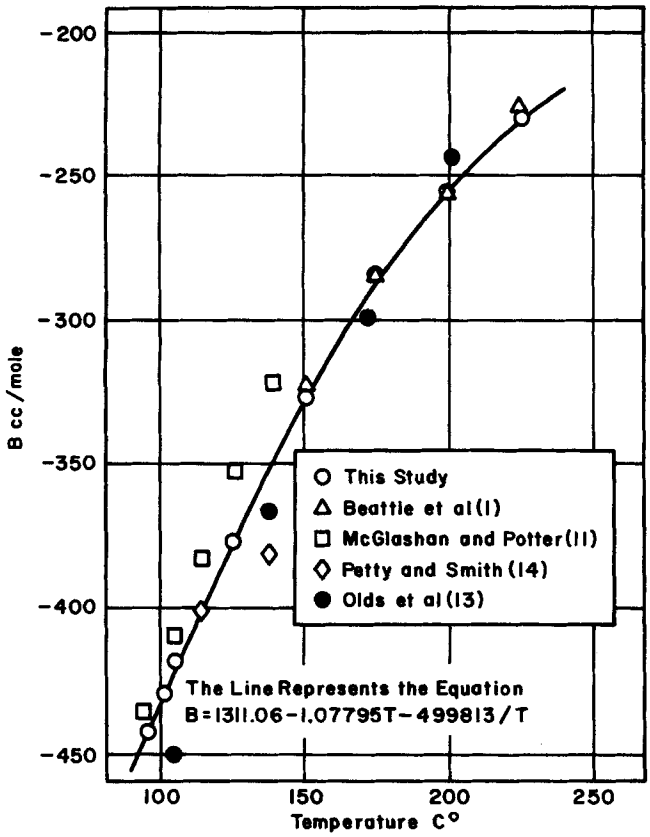

Fig. 2. The second virial coefficient of *n*-butane.

lower temperatures, but the two sets of data diverge as the temperature is raised. The data of other investigators (*13, 14*) show more internal scatter. Recent values of B_{11} reported by Bottomley and Spurling (*3*) at temperatures below 150°C., not shown in Figure 2, fall on a curve about 3% below the present results.

SECOND VIRIAL COEFFICIENTS OF HELIUM–*n*-BUTANE MIXTURES

The second virial coefficients of the 35.3 and 38.3 mole % helium mixtures are given in Table 4. Also shown are the number of moles computed for each isotherm and the precision of the values given in terms of the 95% confidence interval of B_m as determined from a regression analysis.

The second virial coefficient of a binary gas mixture B_m (*10*) is given in terms of the second virial coefficients of the pure components and the mixed second virial coefficient B_{12} by Equation (4):

Table 4. Experimental Values of the Second Virial Coefficients of Helium–*n*-Butane Mixtures

	Mixture No. 1 ($X_2 = 0.353$) Helium			Mixture No. 2 ($X_2 = 0.383$) Helium		
T, °C.	$n \times 10^3$ g.-moles	B_m, cc./g.-mole	−95% C.I.	$n \times 10^3$ g.-moles	B_m, cc./g.-mole	−95% C.I.
100.1	0.26417	−158.5	0.8	0.30811	−139.0	1.1
125.0	0.26424	−134.5	0.8	0.30811	−115.1	1.2
150.0	0.26410	−111.7	1.0	0.30818	−97.9	0.8
175.0	0.26413	−97.0	1.3	0.30793	−81.7	1.0
200.1	0.26418	−84.0	1.7	0.30806	−74.3	0.6
225.1	0.26392	−70.5	1.2	0.30779	−60.4	1.2

Table 5. Experimental Values of B_{12} Helium–*n*-Butane Mixtures

	B_{12}, cc./g.-mole	
T, °C.	Mixture No. 1	Mixture No. 2
100.1	45.0	50.8
125.0	45.5	55.4
150.0	51.9	53.6
175.0	48.5	56.2
200.1	47.4	46.1
225.1	53.0	54.3

$$B_m = X_1^2 B_{11} + 2X_1X_2B_{12} + X_2^2 B_{22} \qquad (4)$$

where X_1 and X_2 are the mole fractions of the pure components. By rearranging Equation (4), B_{12} was calculated from the experimental values of B_m at each temperature, using values of B_{11} obtained from Equation (3) and values of B_{22} obtained from the data of Schneider and Duffie (*17*). The calculated values of B_{12} for the two mixtures are given in Table 5 and are plotted vs. temperature in Figure 3. The precision of these values is estimated as ± 5 cc./g.-mole. It is seen that the values of B_{12} determined from mixture No. 2 (38.3% helium) are, in general, slightly higher than those determined from mixture No. 1. Nevertheless, the agreement in each case is within the estimated uncertainty of the data.

PREDICTED VALUES OF B_{12}

No other experimental values of B_{12} for the helium–*n*-butane system are available for comparison with these results, but values of B_{12} have been predicted by three

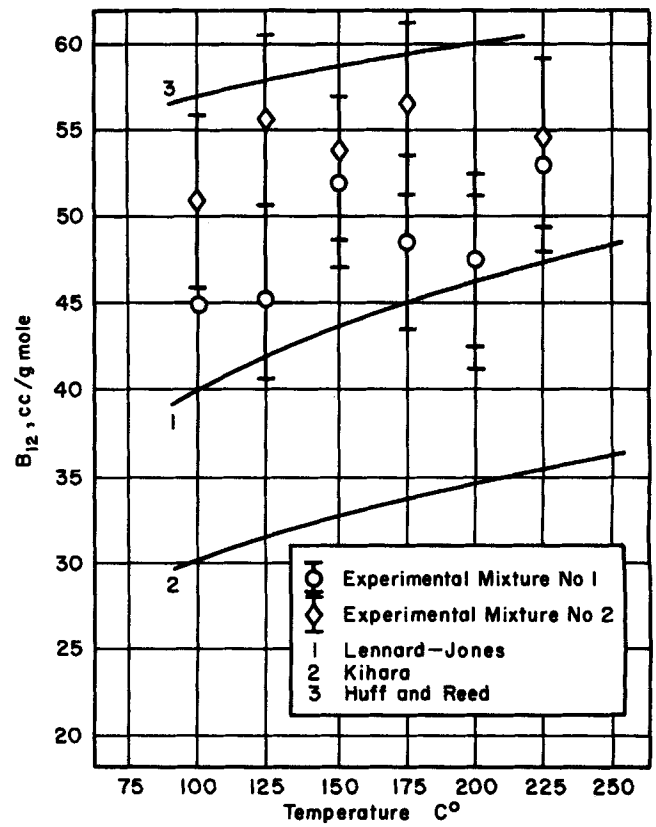

Fig. 3. Variation of B_{12} with temperature calculated by different methods; helium–*n*-butane.

Table 6. Comparison of the Second Virial Coefficient of *n*-Butane Determined from Lennard-Jones Potential Function with Experimental Values

$\epsilon_{11}/k = 270°K.$ $r_{11} = 6.169$ Å.

T, °K.	B_{11} (L-J), cc./g.-mole	B_{11} [Equation(3)], cc./g.-mole
378.0	—407.5	—418.7
391.5	—380.5	—387.6
405.0	—355.7	—359.6
418.5	—332.8	—334.3
432.0	—311.6	—311.6
445.0	—291.9	—291.0
459.0	—273.6	—272.6
472.5	—256.5	—256.0
486.0	—240.5	—241.2
499.5	—225.6	—227.9

Table 7. Calculated Values of B_{12} for the Lennard-Jones Potential Function

$\epsilon_{11}/k = 270°K.$ $r_{11} = 6.169$ Å.
$\epsilon_{22}/k = 10.22°K.$ $r_{22} = 2.556$ Å.
$\epsilon_{12}/k = 52.53°K.$ $r_{12} = 4.363$ Å.

T, °K.	B_{12} (L-J), cc./g.-mole
367.7	39.4
420.2	43.3
472.8	46.2
525.3	48.3

Table 8. Comparison of the Second Virial Coefficient of *n*-Butane Determined from the Kihara Potential Function with Experimental Values

$U_{11}/k = 672.32°K.$ $a_1 = 0.938$ Å. $\rho_{11} = 3.316$ Å.

T, °K.	B_{11} (Kihara), cc./g.-mole	B_{11} [Equation (4)], cc./g.-mole
373.5	—430.8	—429.7
384.2	—404.6	—404.0
395.5	—379.1	—378.9
407.4	—354.7	—354.9
420.2	—331.0	—331.4
433.8	—308.3	—308.7
448.2	—286.2	—287.3
463.7	—264.9	—266.8
480.2	—244.3	—247.4
498.0	—224.4	—229.3

Table 9. Calculated Values of B_{12} for the Kihara Potential Function

$U_{11}/k = 672.32°K.$ $a_1 = 0.938$ Å. $\rho_{11} = 3.316$ Å.
$U_{22}/k = 9.927°K.$ $a_2 = 0.0$ $\rho_{22} = 2.921$ Å.
$U_{12}/k = 81.70°K.$ $a_{12} = 0.469$ Å. $\rho_{12} = 3.119$ Å.

T, °K.	B_{12} (Kihara), cc./g.-mole
371.4	30.0
389.0	31.0
408.5	32.0
430.0	33.0
453.9	33.9
480.6	34.8
510.6	35.7

Table 10. Calculated Value of B_{12} by the Method of Huff and Reed (*6*) Helium–*n*-Butane System

T, °K.	B_{12} (H-R), cc./g.-mole
373.2	56.9
398.2	57.7
423.2	58.5
448.2	59.2
473.2	59.9
498.2	60.4

semiempirical methods based on the pure component properties. These values are plotted in Figure 3. The first method involves fitting Lennard-Jones potential functions to the two pure components and assuming the empirical combining rules (see reference 5, p. 168) to compute the parameters of the mixture potential ϕ_{12}. The Lennard-Jones parameters used for helium are those given in Table I-A of reference 5. The parameters for *n*-butane in this table failed to represent the observed second virial coefficient data. Instead, parameters were determined by fitting the observed data for B_{11}. Table 6 shows the agreement of B_{11} determined with the Lennard-Jones potential using these parameters with experimental values [Equation (3)]. It is seen that the calculated values agree with the experimental values from 405° to 499.5°K. within experimental error. However, the agreement is poor at lower temperatures. Table 7 lists values of B_{12} calculated from the Lennard-Jones potential obtained with the empirical combining rules. These values appear to lie about 5 cc./g.-mole, on the average, below the experimental data. This agreement should probably be considered fortuitous, however, since the Lennard-Jones potential can fit the second virial coefficient data of a real gas only over a limited range of temperatures. Indeed, it does not fit the present data for *n*-butane at the lower temperatures, as shown above.

The second method used to predict B_{12} involves fitting the second virial coefficient of the pure components with Kihara potential functions and using the empirical combining rules to obtain the parameters for ϕ_{12}. The Kihara parameters for helium given by Prausnitz and Myers (*15*) were used, together with values of B_{11} with those predicted with the use of Stewart's parameters, are given in Table 8. The agreement is within experimental error, except at the highest temperature. Predicted values of B_{12} are given in Table 9. Here agreement with experimental values is not good; the predicted values are about 15 cc./g.-mole low. This discrepancy appears to result, not from a failure of the Kihara potential function, which has been extensively used with success for both pure gases and mixtures, but from a breakdown of the empirical combining rules of this case. To fit the data it is apparent that either ρ_{12} must be greater than $\frac{1}{2}$ $(\rho_{11} + \rho_{22})$, or that Stewart's value of ρ_{11} is too small. This latter possibility seems unlikely, however, in view of the excellent fit of the B_{11} data obtained with this used.

The third method used to predict B_{12} is a semiempirical method proposed by Huff and Reed (*8*). Values of B_{12} calculated with this method are given in Table 10. The agreement with the data is good, with the predicted values being about 5 cc./g.-mole high, on the average.

DISCUSSION OF RESULTS

The large relative uncertainty in the experimental values of B_{12} precludes any attempt to specify the dependence

of B_{12} on temperature which is required to determine the parameters for an intermolecular potential function from the data themselves. Nevertheless, the measurements convey significant information regarding intermolecular forces in this system.

The Lennard-Jones potential curves for the system calculated with the parameters in Table 7 are shown in Figure 4. Assuming that these curves approximate those corresponding to the true potential functions, we see that the attractive portions of the ϕ_{22} and ϕ_{12} curves are much shallower than that of ϕ_{11}. This suggests that the system at low concentrations of helium might possible be represented empirically by a model in which a gas composed of hard sphere molecules is dissolved in a real gas, that is, that the 1-2 and 2-2 interactions are hard sphere interactions, while the 1-1 interaction occurs between real gas molecules with a greater attractive well in their potential function ϕ_{11}. The potential function ϕ_{ij} for the interaction between two nonattracting spheres of collis on diameter r_{ij} is given by

$$\phi_{ij}(r) = \infty, r < r_{ij}$$
$$\phi_{ij}(r) = 0, r > r_{ij} \quad (5)$$

By integration of the statistical mechanical equation

$$B(T) = N/2 \int_o^\infty [1 - \exp\{-\phi(r)/kT\}] 4\pi r^2 dr \quad (6)$$

for the interaction of two spherical nonpolar molecules (*6*), the equation for the second virial coefficient is obtained as

$$B^*_{ij} = 2/3\, N\pi r^{*3}_{ij} \quad (7)$$

By this equation, B_{22} and B_{12} are independent of temperature. This is actually a very good approximation in the helium–*n*-butane system over the range of temperatures covered in this study; B_{22} decreases from 11.4 to 11.0 cc./g.-mole between 100° and 225°C. (*17*), while B_{12} (Figure 3) appears to increase but slightly in this interval.

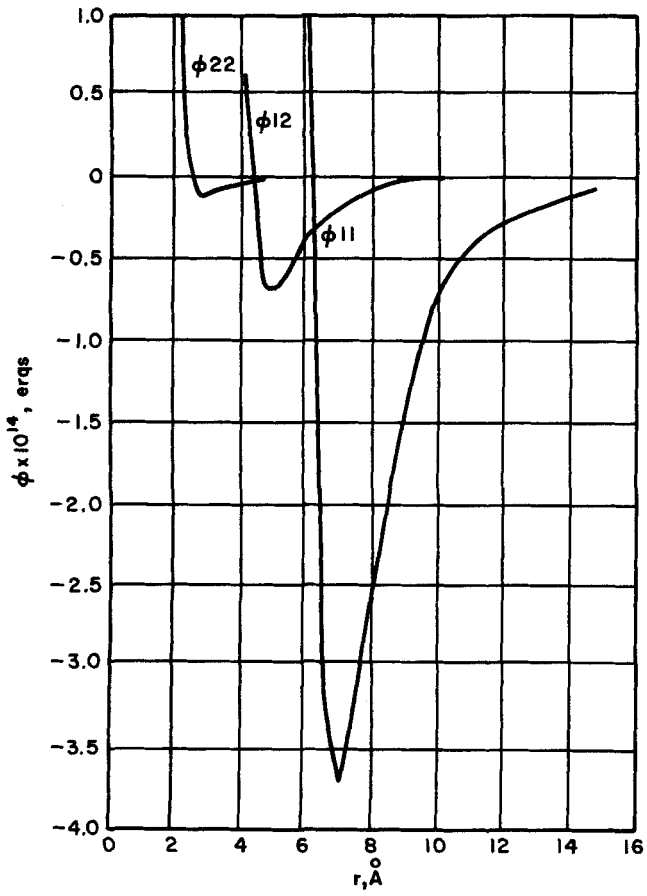

Fig. 4. Lennard-Jones potentials for the helium–*n*-butane system.

To explore further the applicability of an empirical hard sphere–real gas model to the helium–*n*-butane system, an equation of state may be derived for the model based on the general equation of state for binary fluid mixtures (*16*):

$$\frac{P}{kT} = \rho_N - \frac{\rho_N}{6kT} \int_o^\infty \left[X_1^2 g_{11} \frac{\partial \phi_{11}}{\partial r} + 2X_1X_2g_{12} \frac{\partial \phi_{12}}{\partial r} + X_2^2 g_{22} \frac{\partial \phi_{22}}{\partial r} \right] 4\pi r^3 dr \quad (8)$$

Within the spirit of the model, we assume that ϕ_{12}, ϕ_{22}, g_{12}, and g_{22} may be represented by ϕ^*_{12}, ϕ^*_{22}, g^*_{12}, and g^*_{22}, the intermolecular potential energy functions and radial distribution functions for hard sphere interactions, respectively. When values of r^*_{12} and r^*_{22}, the hard sphere collision diameters for the interactions, are available, ϕ^*_{12} and ϕ^*_{22} may be obtained from Equation (5). Then g^*_{12} and g^*_{22} can be computed as functions of composition and density by a procedure described by McLellan and Alder (*12*).

Equation (8) may be integrated for the hard sphere interactions to give

$$\frac{P}{kT} = \rho_N - \frac{\rho_N{}^2 X_1^2}{6kT} \int_o^\infty g_{11} \frac{\partial \phi_{11}}{\partial r} 4\pi r^3 dr + \frac{2\pi \rho_N{}^2}{3} [2X_1X_2 g^*_{12} r^{*3}_{12} + X_2^2 g^*_{22} r^{*3}_{22}] \quad (9)$$

Note that the radial distribution function of the heavy component in the mixture g_{11} depends on the composition of the mixture as well as on the temperature and density. We will assume that there is some density at which the pure heavy component at the temperature of the mixture will have a radial distribution function equal to g_{11}, namely

$$g_1{}^o(\rho_o, T, X_1 = 1.0) = g_{11}(\rho, T, X_1) \quad (10)$$

When Equation (9) is then written for the pure heavy component on a molar basis and rearranged with the aid of Equation (10), the unknown integral may be evaluated:

$$\int_o^\infty g_{11} \frac{\partial \phi_{11}}{\partial r} 4\pi r^3 dr = \frac{6RT}{N\rho_o} \left[1 - \frac{P_o(\rho_o, T)}{\rho_o RT} \right] \quad (11)$$

P_o is the pressure exerted by the *pure* heavy component at density ρ_o and temperature T. By substituting Equation (11) into Equation (9) and simplifying with the aid of Equation (7), we obtain the expression

$$\frac{P}{\rho RT} = 1 - \frac{\rho X_1^2}{\rho_o} \left[1 - \frac{P_o(\rho_o, T)}{\rho_o RT} \right] + \rho [2X_1X_2 g^*_{12} B^*_{12} + X_2^2 g^*_{22} B^*_{22}] \quad (12)$$

B^*_{12} and B^*_{22} are the known second virial coefficients for the hard sphere interactions; g^*_{12} and g^*_{22} are known functions of composition and density; and P_o may be obtained from a valid equation of state for the pure heavy component, after one has chosen a suitable value for

the hypothetical density ρ_o. In the limit as X_1 approaches 1.0, ρ approaches ρ_o. Therefore, we may assume that for mixtures rich in the heavy component, ρ_o may be replaced by ρ. Equation (12) then becomes an equation of state for dilute mixtures of hard sphere molecules in a real gas:

$$P = X_1^2 P_o + X_2 \rho RT \left[1 + X_1 + \rho \left(2X_1 g_{12}^* B_{12}^* + X_2 g_{22}^* B_{22}^*\right)\right] \quad (13)$$

This equation of state was tested by predicting the *PVT* behavior of helium–n-butane mixtures containing 1.89 and 5.03 mole % helium, whose experimentally determined volumetric behavior was reported in Part I. In the computations, B_{12}^* was taken as 50.6 cc./g.-mole, the average of the experimental values in Table 5. B_{22}^* was taken to be 11.2 cc./g.-mole, the mean value of B_{22} between 100° and 225°C. (*17*). Using these values, we find the hard sphere radial distribution functions by the procedure of McLellan and Alder (*12*) to be

$$g_{12}^* = 1 + \rho_N(14.34\,X_1 + 108.44\,X_2) + \tfrac{1}{2}\,\rho_N^2\,(-289.8\,X_1^2 + 280.6\,X_1X_2 + 16980.9\,X_2^2) \quad (14)$$

$$g_{22}^* = 1 + \rho_N(11.59\,X_1 + 93.83\,X_2) + \tfrac{1}{2}\,\rho_N^2\,(155.0\,X_1^2 + 2648.0\,X_1X_2 + 17286.8\,X_2^2) \quad (15)$$

The Benedict-Webb-Rubin equation of state for *n*-butane (*2*) was used to compute P_o. Under all conditions of temperature (144.7° to 183.6°C.) and density (up to 1.5 times the critical density) the maximum deviation between the calculated and observed pressures for the mixtures was 2.9%. By comparison, deviations as high as 12% were obtained with the Beattie-Bridgeman equation of state using the empirical relations suggested by Dodge (*4*) for the mixture parameters. Thus Equation (13), a semiempirical equation of state for mixtures of hard sphere molecules and a real gas, gives a very good representation of the PVT behavior of helium–*n*-butane mixtures in the region of low helium concentrations.

Additional PVT data at higher helium concentrations and higher densities would be desirable to determine the limits of applicability of Equation (13). In addition, the hard sphere–real gas model would be expected to apply to dilute mixtures of helium and other heavier fluids; the method of Huff and Reed (*8*) is recommended to estimate B_{12}^* in the absence of experimental data. Extension of this model to helium-bearing natural gases is suggested.

ACKNOWLEDGMENT

Grateful acknowledgment is made to the American Oil Company, the National Science Foundation, and The Ohio State University for financial aid in the form of fellowships and a research assistantship to A. E. Jones; to the Helium Research Center, Bureau of Mines, for the helium; and to the Phillips Petroleum Company for the *n*-butane. The authors wish to thank the staff of the Numerical Computation Laboratory of The Ohio State University for assistance in preparing the computer programs used in this study.

NOTATION

B_{ij} = second virial coefficient representing the interaction of molecules of species *i* and *j*, cc./g.-mole
B_{ij}^* = second virial coefficient representing the interaction of hard sphere molecules *i* and *j*, cc./g.-mole
B_m = second virial coefficient of gas mixture, cc./g.-mole
C = third virial coefficient, cc.^{2}/g.-mole^2
g_{ij}^* = radial distribution function for hard sphere component pair *i*, *j*, dimensionless
k = Boltzmann's constant, (atm.)(cc.)(molecule)$^{-1}$(°K.)$^{-1}$
N = Avogadro number
n = sample mass, g.-moles
P = pressure, atm. unless otherwise indicated
R = gas constant, (atm.)(cc.)(g.-mole)$^{-1}$(°K.)$^{-1}$
r = distance between molecular centers, Å.
r_{ij} = length parameter in Lennard-Jones potential representing the *i-j* interaction, Å.
r_{ij}^* = hard sphere collision diameters, Å.
T = temperature, °K. where not otherwise indicated
U_{ij} = energy parameter of Kihara potential representing the *i-j* interaction, (atm.)(cc.)(molecule)$^{-1}$
V = sample volume, cc.
X_i = mole fraction of component *i*, dimensionless
y_i = quantity defined by Equation (2), cc./g.-mole

Greek Letters

ϵ_{ij} = energy parameter for Lennard-Jones potential representing the *i-j* interaction, (atm.)(cc.)(molecule)$^{-1}$
ρ = density, g.-mole/cc.
ρ_{ij} = length parameter in Kihara potential representing the *i-j* interaction, Å.
ρ_N = number density, molecules/cc.
ρ_o = hypothetical density as defined in Equation (10), g.-moles/cc.
ϕ_{ij} = potential energy function representing the interaction of molecules of species *i* and *j*, ergs

LITERATURE CITED

1. Beattie, J. A., G. L. Simard, and Jouq-Jen Su, *J. Am. Chem. Soc.*, **61**, 24 (1939).
2. Benedict, M., G. B. Webb, and L. C. Rubin, *Chem. Engr. Progr.*, **47**, 419 (1951).
3. Bottomley, G. A., and T. H. Spurling, *Australian J. Chem.*, **17**, 501 (1964).
4. Dodge, B. F., "Chemical Engineering Thermodynamics," p. 198, McGraw-Hill, New York (1944).
5. Hirschfelder, J. O., C. F. Curtiss, and R. B. Bird, "Molecular Theory of Gases and Liquids," Chap. 3, Wiley, New York (1954).
6. *Ibid.*, p. 150.
7. Hirschfelder, J. O., F. T. McClure, and I. F. Weeks, *J. Chem. Phys.*, **10**, 201 (1942).
8. Huff, J. A., and T. M. Reed III, *J. Chem. Eng. Data*, **8**, 306 (1963).
9. Jones, A. E., Ph.D. dissertation, Ohio State Univ., Columbus (1964); Dissertation Abstracts Order No. 65-1192. Microfilm $3.05. University Microfilms, Inc., 313 N. 1st St., Ann Arbor, Mich.
10. Mayer, J. E., *J. Phys. Chem.*, **43**, 71 (1939).
11. McGlashan, M. L., and D. J. B. Potter, *Proc. Roy. Soc. (London)*, **A267**, 478 (1962).
12. McLellan, A. G., and B. J. Alder, *J. Chem. Phys.*, **24**, 115 (1956).
13. Olds, R. H., H. H. Reamer, B. H. Sage, and W. N. Lacey, *Ind. Eng. Chem.*, **36**, 282 (1944).
14. Petty, L. B., and J. M. Smith, *ibid.*, **47**, 1258 (1955).
15. Prausnitz, J. M., and A. L. Meyers, *AIChE J.*, **9**, 5 (1963).
16. Rushbrooke, G. S., and H. L. Scoins, *Phil. Mag. Ser.*, **7**, 42, 582 (1951).
17. Schneider, W. G., and J. A. H. Duffie, *J. Chem. Phys.*, **17**, 751 (1949).
18. Stewart, W. E., private communication.

Manuscript received August 4, 1965; revision received November 14, 1966; paper accepted November 14, 1966.